Adaptive Output Feedback Force Tracking Control for Lower Extremity Power-Assisted Exoskeleton

Shengli Song*, Yuxuan Cao *, Haitao Wang*, Jinhong Xue*, Xinglong Zhang *, Junyong Fu, Fangwen Tu*****

** Army Engineering University of PLA, Nanjing, 210007, China.*
(e-mail:yuxuanCaoPLA@163.com)
*** Shanghai Key Laboratory of Space Intelligent Control Technology Shanghai, 201108, China.*
**** National University of Singapore, 117576, Singapore.*

Abstract: This paper presents an output feedback adaptive force tracking control scheme for Lower Extremity Power-assisted Exoskeleton (LEPEX). LEPEX is driven by electro-hydraulic actuators geometrically mounted for the active joints, which exhibits high nonlinear dynamics. In view of this, a robust observer resorting to Radius Basis Function Neural Network (RBF-NN) is proposed to approximate the nonlinearities so as to detect the values of the process variables. An adaptive controller compatible with the RBF-NN estimator is adopted to cope with the nonlinearities and possible model uncertainties. The convergence of the output, i.e., load force variable, to a computable set is guaranteed in the context of Lyapunov direct method. Finally, simulation and experimental tests on the force control of an ankle joint of LEPEX are studied to witness the potentiality of the proposed approach.

Keywords: low extremity exoskeleton, hydraulic driving system, neural network, adaptive control, output feedback control.

1. INTRODUCTION

Nowadays, heavy loads are usually transported with wheeled vehicles due to their adequate load-carrying capability. However, wheeled vehicles are not suitable for the rugged terrains and/or the needs to move up and/or down stairs. For these reasons, the developments of legged locomotion become more attractive over the last decades, see (Zoss et al., 2006; Chu et al., 2005; Ghan and Kazerooni, 2006; Gupta et al., 2008). Among them, lower extremity exoskeleton is a legged locomotive humanoid robot, which is used for helping soldiers bear heavy loads so as to increase their load capacity and improve their flexibility, and for assisting elderlies and patients who experience dificulties in their movability, to fulfil the daily living movements, see (Banala et al., 2009; Li et al., 2013).

A Lower Extremity Power-assisted Exoskeleton (LEPEX) is presented in Fig. 1, where each leg has 7 degrees of freedom (d.o.f.), among which, 3 d.o.f is allowed at the hip joint, 1 d.o.f is enabled at the knee joint, while the other 3 ones are employed at the ankle joint. Among them, the d.o.f. of the knee and ankle joints in the sagittal plane are active ones. Each active joint is driven by an actuator that must provide power in real time to reduce wear’s energy consumption. Hence, control of the hydraulic actuators (joints) is vital to achieve high level human-machine interaction performance.

Force control is widely used in power augmentation exoskeleton robot due to the fact that it implicitly guarantees a safe and smooth operation for human-robot interaction (Lee et al., 2012). In recent years, literatures related with force tracking control goal for hydraulic driving systems have been reported, see (Alleyne and Liu, 2000; Kilic et al., 2012; Steger, 2005), but it has been noticed that force perception that provides precise and repeatable measurements in terms of human lower extremity exoskeleton is still difficult and costly, see (Ho and Ahn, 2010; Kazerooni et al., 2005; Pan et al., 2014; Rito et al., 2006). In (Kazerooni and Steger, 2006), a virtual force/torque control algorithm has been developed where only indirect measurement of the external force is required. A robust integral admittance shaping approach has been addressed in (Nagarajan et al., 2016) for active exoskeleton with parameter uncertainties. It has been proven that neural network (NN) is capable to approximate nonlinearities globally without a priori the structure of the system, see (Jagannathan, 2006; Park and Han, 2010; Huang et al., 2013; Ge and Wang, 2014). The methods have been extended to the application to estimation of robot dynamics with NN, see (Ge et al., 2009; Kazerooni and Steger, 2006). An observer for nonlinear system based on NN has also been developed with resorting to back propagation, see (Abdollahi et al., 2006; Sharma and Verma, 2012; Sharma and Verma, 2013; Li et al., 2013; Huang and Jiang, 2015).

In this paper, an output feedback adaptive force tracking control scheme with NN observer is developed for LEPEX. First, a dynamic model describing the open-loop hydraulic driving system and geometric structure of the robot is established which shows high nonlinear dynamics. A multilayer feedforward Radius Basis Function Neural Network (RBF-NN) observer is proposed to approximate the nonlinearities so as to estimate the states, such as force of load F_L , valve spool position x_v . An adaptive controller compatible with the RBF-NN estimator is developed to cope with the nonlinearities and possible model uncertainties. The convergence of the output, i.e., load force variable, to a computable set is guaranteed in the context of Lyapunov direct method. Finally, simulation and experimental tests on the force control of an ankle joint of LEPEX are studied to witness the potentiality of the proposed scheme. The contributions of this paper are twofold: 1) Compared with the existing method, see (Ho and Ahn, 2010; Kazerooni et al., 2005; Pan et al., 2014; Rito et al., 2006; Kazerooni and Steger, 2006), the proposed approach relies on a robust observer, which allows to estimate the external force without the use of multi-dimensional force sensors; 2) The system is a slightly improved version of the one in (Song et al., 2014), while the proposed control algorithm shows a huge improvement especially in its capability to deal with nonlinearities and model uncertainties. Note that, for simplicity the force control of only one joint, i.e., the right or left ankle joint, is considered as the study example in this paper.

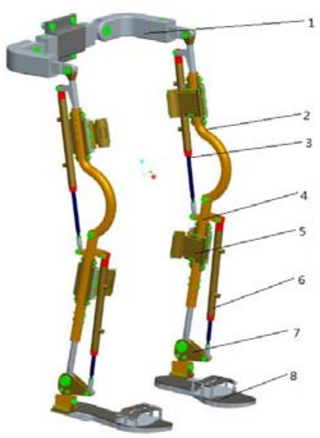

Fig. 1. Structure of the LEPEX 1-Hip 2-Thigh 3 Thigh Drive Cylinder 4-Shank 5-Bound Device 6-Shank Drive Cylinder 7-Ankle 8-Sole.

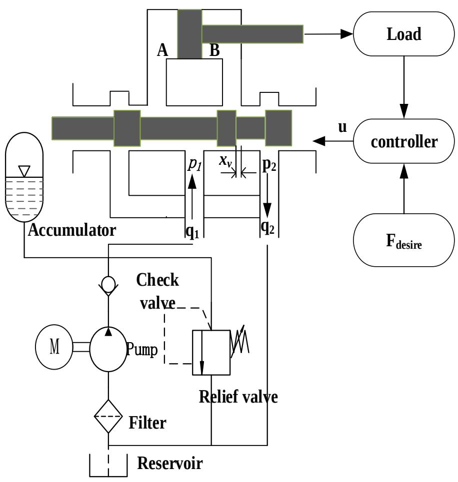

Fig. 2. The principle diagram of hydraulic driving model.

The rest of this work is presented as follows: Section 2 introduces the description of hydraulic driving model. Section 3 describes the RBF-NN based observer and the adaptive controller as well as their theoretical properties. Section 4 presents the simulation and experiment results while Section 5 concludes the paper.

2. DESCRIPTION OF THE MODEL

The hydraulic driving system (see Fig. 2) is made by a pump, a servo-valve, a cylinder, a relief valve, a check valve, a reservoir, an accumulator, a filter and other auxiliary components. The pump in the system is adopted to produce high pressure fluid for driving the hydraulic cylinder. The accumulator is introduced to provide the emergency stop or the opening of the flow system once it encounters urgent events. The relief valve is in charge of guaranteeing constant pressure of the pump. The operation principle of hydraulic driving system is as follows. The voltage signal is regarded as the control action of the system, while the spool displacement and force of the cylinder are chosen as the corresponding controlled variables. In the system, the spool and the cylinder form a feedback connection. Cylinder displacement can accurately react as the spool displacement varies, in this way the input of mechanical quantity is transformed into a large value of output force. Therefore, in view of this, the system is seen as a power amplifying device. The opening degree of the spool changes based on the voltage variations resulting from the regulator, in this way the values of pressure and the flow rate varies accordingly.

The state space representation of the hydraulic driving model can be given as, see (Song et al., 2014)

$$\begin{cases} \ddot{\varphi} = \dfrac{1}{J}[M(F_L + F_f) - mgr\sin(\varphi)] \\ \dot{F}_L = n_1 x_v - n_2 \dot{x}_c - n_3 F_L + n_4 \\ \dfrac{dx_v}{dt} = \dfrac{1}{\tau}(k_s u - x_v) \end{cases} \tag{1}$$

where

$$F_L = A_1 p_A - A_2 p_B$$

$$n_1 = \frac{\beta(A_1 + A_2)K_q}{V_0}$$

$$n_2 = \frac{\beta(A_1 + A_2)^2}{2V_0}$$

$$n_3 = \frac{\beta(2K_c + C_{in} + C_{ec})}{V_0}$$

$$n_4 = \frac{\beta(2K_c + C_{in} + C_{ec})(A_2 - A_1)}{2V_0} p_s$$

In (1), φ is the joint angle of LEPEX, J is the system inertia, M is the moment arm related to ankle joint, F_L is the load force, F_f is the friction force caused by the interaction of the piston and the cylinder, m and r are the mass and the mass center, x_v is the spool displacement, $\dot{x}_c$ is the derivative of the position displacement, τ is the mechanical time constant of the spool, k_s is the DC gain of the valve voltage to the spool position, u is control variable, A_1 and A_2 are the areas of piston corresponding to A and B, p_A and p_B are the pressure of room A and B， C_{in} and C_{ec} are the hydraulic internal and external leakage of the system, V_0 is initial volume of cylinder respectively.

3. RBF-NN OBSERVER BASED ADAPTIVE CONTROLLER DESIGN

In this section, the RBF-NN based observer is initially designed to estimate the state variable of (1). Based on this observer, a NN network based back-stepping controller is introduced in order to deal with nonlinearities and model uncertainties.

3.1 RBF-NN observer Design

In this section, a three-layer RBF-NN estimator is developed to approximate the variables, e.g., F_L and x_v of system (1). To this end, first let z be $\left[F_L \quad x_v\right]^T$, and from system (1) we also define

$$F(z,u)=\begin{bmatrix} n_1x_v - n_2\dot{x}_c - n_3F_L + n_4 \\ \frac{1}{\tau}k_s u - \frac{1}{\tau}x_v \end{bmatrix} \tag{2}$$

Then, by adding and subtracting Az , from (1) one can write

$$\begin{aligned} \dot{z}(t) &= Az + G(z,u) \\ y(t) &= Cz(t) \end{aligned} \tag{3}$$

where $G(z,u)=F(z,u)-Az$, A is selected such that A is Hurwitz stable and the pair $(C,\ A)$ is observable.

Therefore, the state observer of the system (1) can be described as

$$\begin{aligned} \dot{\hat{z}}(t) &= A\hat{z} + \hat{G}(z,u) + L(y - C\hat{z}) \\ \hat{y} &= C\hat{z}(t) \end{aligned} \tag{4}$$

where $\hat{z}$ and $\hat{y}$ are the estimated state and output variables respectively. $L \in R^{2\times 1}$ is the observer gain, and the selection of L must satisfy that matrix $A - LC$ is Hurwitz stable.

It has been noted that a three-layer RBF-NN with only one single-hidden layer is sufficient to approximate any degree of nonlinear system, see (Ge et al., 2009; Igelnik and Pao, 1995; Jagannathan, 2006; Lewis et al., 1999; Lewis and Vrabie, 2009; Xiong et al., 2014). For this reason, according to the approximation principle of RBF-NNs, $G(z,u)$ can be described by

$$G(z,u) = WS_1\left(H\bar{z}\right) + \varepsilon(z) \tag{5}$$

where W and H are the corresponding weight matrices of the output and hidden levels, $\bar{z} = \left[z^T, \quad u^T\right]^T$ is the input to be applied to the NN observer, ε is the NN functional approximation error, and it is bounded, i.e., $|\varepsilon| \le \varepsilon_0$, ε_0 is a small positive scalar and in principle can be arbitrarily small by adjusting the structure of the NNs, $S_1(\cdot)$ is the NN activation function.

Assume that perfect weights W is bounded with a finite constant, that is

$$\|W\| \le W_M \tag{6}$$

where $\|\cdot\|$ represent the Euclidean norm.

The nonlinear function $G(z,u)$ can be approximated by

$$\hat{G}(\hat{z},u) = \hat{W}S_1\left(H\hat{\bar{z}}\right) \tag{7}$$

where $\hat{z}$ is the estimated state vector, $\hat{\bar{z}} = \left[\hat{z}^T, \quad u^T\right]^T$, $\hat{W}$ is the estimate of the perfect weights vector.

Then, the dynamics of NN observer can be described by

$$\begin{aligned} \dot{\hat{z}}(t) &= A\hat{z} + \hat{W}S_1(H\hat{\bar{z}}) + L(y - C\hat{z}) \\ \hat{y}(t) &= C\hat{z}(t) \end{aligned} \tag{8}$$

We define $\tilde{z} = z - \hat{z}$ and $\tilde{y} = y - \hat{y}$, where $\tilde{z}$ and $\tilde{y}$ are the state and output estimation errors, then from (4), (5) and (8), the dynamics resulted from the deviation of (8) and (3) can be obtained as

$$\begin{aligned} \dot{\tilde{z}}(t) &= Az + WS_1(H\bar{z}) - A\hat{z} - \hat{W}S_1(H\hat{\bar{z}}) - L(Cz - C\hat{z}) + \varepsilon\left(z\right) \\ \tilde{y}(t) &= C\tilde{z}(t) \end{aligned} \tag{9}$$

By adding and subtracting $WS_1(H\hat{\bar{z}})$ in (9), we define $\tilde{W} = W - \hat{W}$, $A_c = A - LC$, then (9) can be rewritten as

$$\begin{aligned} \dot{\tilde{z}}(t) &= A_c\tilde{z} + \tilde{W}S_1(H\hat{\bar{z}}) + \zeta\left(t\right) \\ \tilde{y}(t) &= C\tilde{z}(t) \end{aligned} \tag{10}$$

where $\zeta\left(t\right) = W\left[S_1(H\bar{z}) - S_1(H\hat{\bar{z}})\right] + \varepsilon(z)$ is a bounded disturbance term.

Inspired by (Abdollahi et al., 2006), an improved weight updating law proposed for the NN observer is described as follows:

$$\dot{\hat{W}} = -\eta(\tilde{y}^T C A_c^{-1})^T S_1^{\,T}(H\hat{\bar{z}}) - \theta\|\tilde{y}\|\hat{W} \tag{11}$$

where $\Gamma(H\hat{\bar{z}}) = diag\{S_{1j}^2(H\hat{\bar{z}})\},\ j = 1,\quad 2,\quad \cdots,\quad m,$ $\operatorname{sgn}(\hat{\bar{z}}) = \left[\operatorname{sgn}(\hat{\bar{z}}_1),\quad \operatorname{sgn}(\hat{\bar{z}}_2),\quad \operatorname{sgn}(\hat{\bar{z}}_3)\right]^T$ with

$$\operatorname{sgn}(\hat{\bar{z}}_k) = \begin{cases} 1, & for\ \hat{\bar{z}}_k > 0 \\ 0, & for\ \hat{\bar{z}}_k = 0 \\ -1, & for\ \hat{\bar{z}}_k < 0 \end{cases} \tag{12}$$

where $k = 1,2,3$, and $\eta > 0$ is the learning rate, θ is the designed positive number.

Theorem 1. Under the weight adjustment algorithm (11), there exit a computable positive scalar d such that the estimation error of z is uniformly ultimately bounded, i.e., $\|\tilde{z}\| \le d$.

Proof: see reference (Abdollahi et al., 2006).

3.2 Adaptive NN controller design

Let $x_1 = F_L, x_2 = \dot{F}_L$, from system (1) one has

$$\begin{aligned} \dot{x}_1 &= x_2 \\ \dot{x}_2 &= \frac{n_1 k_s}{\tau} u - \frac{n_1}{\tau} x_v - n_2 \ddot{x}_c - n_3 (n_1 x_v - n_2 \dot{x}_c - n_3 F_L + n_4) \end{aligned} \tag{13}$$

Assume that a reference trajectory be $x_r(t)$ and define a generalized tracking error as $z_1(t) = x_1(t) - x_r(t)$ and have $\dot{z}_1(t) = x_2(t) - \dot{x}_r(t)$. Another error variable $z_2(t)$ is defined by introducing a virtual control $\alpha_1(t)$, that is $z_2(t) = x_2(t) - \alpha_1(t)$. The virtual control α_1 is selected as

$$\alpha_1 = -K_1 z_1 + \dot{x}_r \tag{14}$$

where the gain matrix $K_1 > 0$. Therefore, one promptly has

$$\begin{aligned} \dot{z}_1 &= z_2 + \alpha_1 - \dot{x}_r = z_2 - K_1 z_1 \\ \dot{z}_2 &= \frac{n_1 k_s}{\tau} u - \frac{n_1}{\tau} x_v - n_2 \ddot{x}_c - n_3 (n_1 x_v - n_2 \dot{x}_c - n_3 F_L + n_4) - \dot{\alpha}_1 \end{aligned} \tag{15}$$

Under (15), we recall the possibility that the model parameters might not be known a-priori. A feedback control policy u can be selected as

$$u = -\frac{\hat{\tau}}{\hat{n}_1 \hat{k}_s} (\hat{z}_1 + K_2 \hat{z}_2) + \hat{f} \tag{16}$$

Where

$$\hat{f} = \frac{1}{\hat{k}_s} x_v + \frac{\hat{n}_2 \hat{\tau}}{\hat{n}_1 \hat{k}_s} \ddot{x}_c + \frac{\hat{n}_3 \hat{\tau}}{\hat{n}_1 \hat{k}_s} (\hat{n}_1 x_v - \hat{n}_2 \dot{x}_c - \hat{n}_3 F_L + \hat{n}_4) + \frac{\hat{\tau}}{\hat{n}_1 \hat{k}_s} \alpha_1$$

where $\hat{t}$ is the measured value of the general variable t .

With (16), uncertainties might be introduced into the second line in (15) due to the possibly inaccurate measurement of the model parameters, that is

$$\Delta = \frac{n_1 k_s}{\tau} (f - \hat{f}) \tag{17}$$

where

$$f = \frac{1}{k_s} x_v + \frac{n_2 \tau}{n_1 k_s} \ddot{x}_c + \frac{n_3 \tau}{n_1 k_s} (n_1 x_v - n_2 \dot{x}_c - n_3 F_L + n_4) + \frac{\tau}{n_1 k_s} \alpha_1$$

In order to compensate for uncertainties in (17), we employ a critic NN to approximate the system. The feedback control u is designed as

$$u = -\frac{\hat{\tau}}{\hat{n}_1 \hat{k}_s} (\hat{z}_1 + K_2 \hat{z}_2) + \hat{W}_c^T S_2(Z) \tag{18}$$

where the gain matrix $K_2 > 0$, $\hat{W}_c$ is the weight matrix, $S_2(Z)$ is the basis function in vector form, $Z = [\hat{x}_v, \dot{\alpha}_1]$ is the input to be applied to the adaptive NN and where $\hat{x}_v$ is the estimated value of x_v . The NN with estimated weights, i.e., $\hat{W}_c^T S_2(Z)$ approximates the optimal estimation $W_c^{*T} S_2(Z)$ which is described in the form

$$W_c^{*T} S_2(Z) = f_c - \varepsilon_c(Z) \tag{19}$$

Where $f_c = \alpha f$, $\alpha = \frac{\hat{\tau}}{\hat{n}_1 \hat{k}_s} \frac{n_1 k_s}{\tau}$, $\varepsilon_c(Z)$ is the approximation error and $\varepsilon_c(Z) \le \bar{\varepsilon}$, $\bar{\varepsilon}$ is a positive scalar which also depends on the value of ε and ε_0 .

The NN adaptive law is developed as (He et al., 2015)

$$\dot{\hat{W}}_c = -\Gamma (S_2(Z) \hat{z}_2 + \sigma \hat{W}_c) \tag{20}$$

where Γ is the gain matrix, a constant, σ is a small constant, $\sigma > 0$.

In order to verify the stability of the NN, a Lyapunov function candidate is chosen, that is

$$V_2 = \frac{1}{2} z_1^2 + \frac{1}{2\alpha} z_2^2 + \frac{1}{2} \tilde{W}_c^T (\alpha T)^{-1} \tilde{W}_c \tag{21}$$

where $\tilde{W}_c = W_c^* - \hat{W}_c$.

Theorem 2. Under control law (18), weight adjustment algorithm (20) and the condition that $K_2 > 1$, then the states of system (15) is uniformly ultimately bounded within a computable set $\Omega = \{z \mid z^T K z \le r\}$, where K is defined in (27).

Proof:

$$\begin{aligned} \dot{V}_2 &= z_1(z_2 - K_1 z_1) + \frac{z_2}{\alpha} (\frac{n_1 k_s}{\tau} (u - f_c)) + \tilde{W}_c^T (\alpha T)^{-1} \dot{\tilde{W}}_c \\ &= z_1 z_2 - K_1 z_1^2 + z_2(-\hat{z}_1 - K_2 \hat{z}_2 + \alpha^{-1} \hat{W}_c^T S_2(Z) - f) + \tilde{W}_c^T (\alpha T)^{-1} \dot{\tilde{W}}_c \\ &= \tilde{z}_1 z_2 - K_1 z_1^2 - K_2 z_2 \hat{z}_2 - \alpha^{-1} z_2 (\tilde{W}_c^T S_2(Z) - \varepsilon_c(Z)) + \tilde{W}_c^T (\alpha T)^{-1} \dot{\tilde{W}}_c \\ &= \tilde{z}_1 z_2 - K_1 z_1^2 - K_2 z_2 \hat{z}_2 + \alpha^{-1} z_2 \varepsilon_c(Z) + \tilde{W}_c^T (\alpha T)^{-1} (\dot{\tilde{W}}_c - \Gamma S_2(Z) z_2) \\ &= \tilde{z}_1 z_2 - K_1 z_1^2 - K_2 z_2 \hat{z}_2 + \alpha^{-1} (z_2 \varepsilon_c(Z) + \tilde{W}_c^T S_2(Z) \tilde{z}_2 + \tilde{W}_c^T \sigma \hat{W}_c) \end{aligned} \tag{22}$$

where $\tilde{z}_1 = z_1 - \hat{z}_1$ and $\tilde{z}_2 = z_2 - \hat{z}_2$.

Taking into account that $\tilde{z}_1 z_2 \le 1/2\, \tilde{z}_1^2 + 1/2\, z_2^2$ and $-K_2 z_2 \hat{z}_2 = -K_2 z_2^2 + K_2 z_2 \tilde{z}_2 \le -(K_2 + 1/2) z_2^2 + 1/2\, K_2^2 \tilde{z}_2^2$, then

$$\begin{aligned} \dot{V}_2 \le & -K_1 z_1^2 - (K_2 - 1) z_2^2 + 1/2\, \tilde{z}_1^2 + 1/2\, K_2^2 \tilde{z}_2^2 \\ & + \alpha^{-1} (z_2 \varepsilon_c(Z) + \tilde{W}_c^T S_2(Z) \tilde{z}_2 + \tilde{W}_c^T \sigma \hat{W}_c) \end{aligned} \tag{23}$$

By completion of squares, one has

$$\begin{aligned} & \tilde{W}_c^T \sigma \hat{W}_c \le \tilde{W}_c^T \sigma (W_c^* - \tilde{W}_c) \\ & \le -\sigma \left\| \tilde{W}_c \right\|^2 + \sigma \left\| W_c^* \right\| \left\| \tilde{W}_c \right\| \end{aligned} \tag{24}$$

and

$$\tilde{W}_c^T S_2(Z) \tilde{z}_2 \le \frac{1}{2} \tilde{z}_2^2 + \frac{1}{2} \left\| S_2(Z) \right\| \left\| \tilde{W}_c \right\| \tag{25}$$

Define $K_{20} > 0$ and $K_{21} > 0$ such that $K_{20} = K_2 - 1 - K_{21}$, then

$$-K_{21}z_2^2 + z_2\alpha^{-1}\varepsilon_c(Z) \le \frac{(\alpha^{-1}\bar{\varepsilon})^2}{4K_{21}} \tag{26}$$

Therefore, from (21) and in view of (22-24), it follows that

$$\dot{V}_2 \le -K_1 z_1^2 - K_{20} z_2^2 + r \tag{27}$$

where

$$r = \alpha^{-1}(-\sigma\|\tilde{W}_c\|^2 + \sigma\|W_c^*\|\|\tilde{W}_c\| + 1/2\|S_2(Z)\|\|\tilde{W}_c\|) + 1/2\,\tilde{z}_1^2 + 1/2(K_2^2+1)\tilde{z}_2^2 + (\alpha^{-1}\bar{\varepsilon})^2/4K_{21}.$$

Recalling that $K_2 > 1$, the state z_1 and z_2 is uniformly ultimately bound in the set $\Omega = \{z \mid z^T K z \le r\}$, where $z = [z_1 \quad z_2]^T$ and

$$K = \begin{bmatrix} K_1 & 0 \\ 0 & K_{20} \end{bmatrix} \tag{28}$$

Remark 1. From Theorem 2, it is evident that larger values of K_1 and K_{20} lead to a faster convergence of the state variable z to the set Ω, while a larger value of K_2 and smaller values of K_{21} and α could result in a larger amplitude of the set Ω. Hence, in order to achieve satisfactory control performance (e.g., fast convergence and small robust set), it is advisable to select larger values of K_1, K_{20}, K_{21} and α, and small values of K_2.

Remark 2. The parameter σ and $\bar{\varepsilon}$ affects the radius of the set Ω and in principle can be set arbitrarily small. In case σ is chosen such that $\sigma \to 0$ and the number of neurons of the observer and the adaptive controller increases until $\bar{\varepsilon} \to 0$, then it follows that $[\tilde{z}_1, \tilde{z}_2]^T \to 0$ and $\tilde{W}_c \to 0$. Consequently, the state z_1 and z_2 converge to the origin.

4. SIMULATION AND EXPERIMENT STUDY

In order to verify the validity of the adaptive output feedback force tracking control algorithm, simulation and experimental tests have been employed, and the corresponding results are reported and analyzed in this section.

4.1 Simulation

The diagram of force adaptive NN tracking controller with NN observer for LEPEX is shown in Fig. 3. During the simulation, the sampling period is selected as 0.001s. The desired force is set as $F_{Ld} = 200 \times \sin(3\pi t)$.

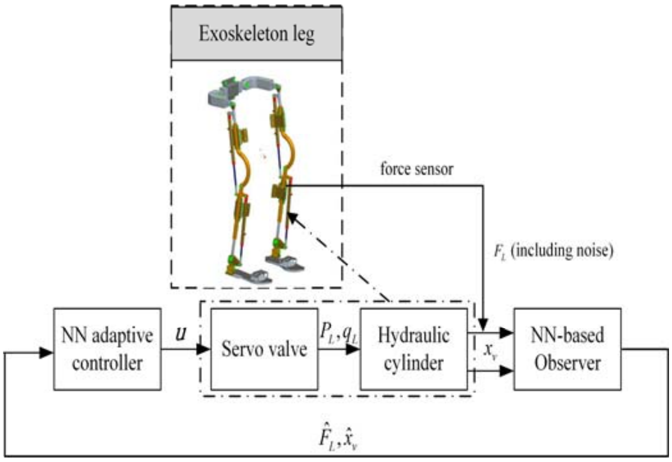

Fig. 3. Diagram of force adaptive NN tracking control scheme with NN observer.

The structure and parameters of the NN observer and adaptive NN force tracking controller are described in Table 1. Note that, as shown in Table 1, two NN structures are designed : a three-layer NN with a single-hidden layer containing sixteen neurons is employed to construct the RBF-NN observer, and an adaptive NN three-layer NN with a single-hidden layer and containing 256 neurons is adopted for the adaptive regulator to compensate for the system uncertainties. The values of the vital parameters of the hydraulic driving system are given in Table 2. The simulation results have been reported in Fig. 4-7, where Fig. 4 depicts the tracking trajectories with desired force of $F_{Ld} = 200 \times \sin(3\pi t)$, Fig. 5 is rectangular area marked in Fig. 4, Fig. 6 gives the deviation of the actual force and the desired one, while Fig. 7 describes the control signal during the force tracking control.

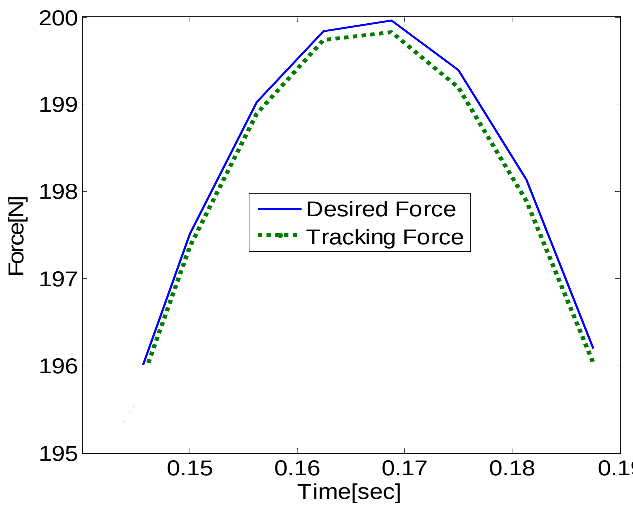

Fig. 4. Tracking trajectories with desired force of $F_{Ld} = 200 \times \sin(3\pi t)$.

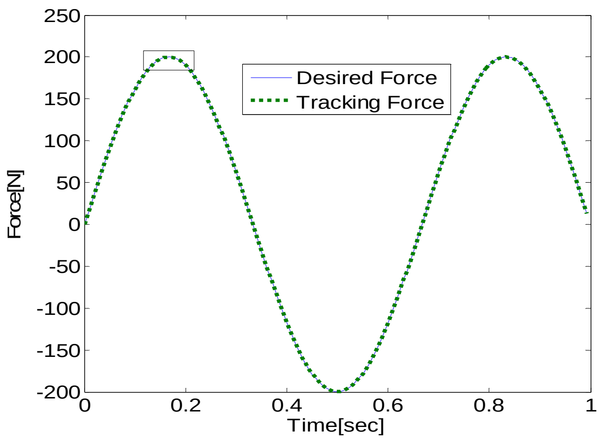

Fig. 5. The rectangular area marked in Fig. 4.

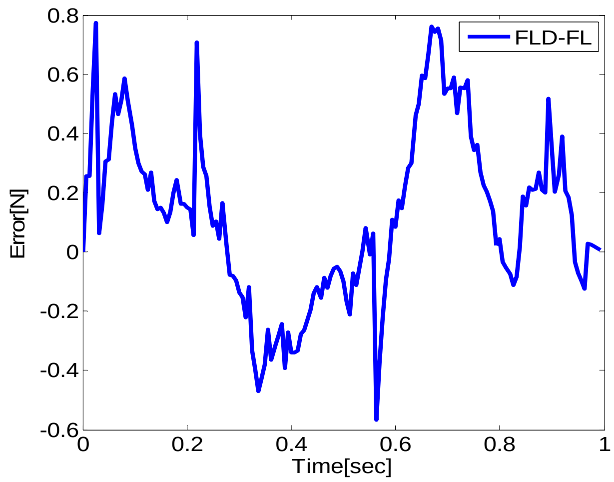

Fig. 6. The force tracking error.

It has been shown from Fig. 6 that the maximum force tracking error is 0.774N. Considering the maximal amplitude of the force reference being 250N, the simulation results indicate that the closed-loop control system exhibits an outstanding force tracking performance.

Table 1. Structure and parameters of the observer and controller.

	NN-observer	Adaptive controller
Type of NN	RBF-NN	RBF-NN
Number neurons	16	256
Learning rate	$\eta = 45$	$\Gamma_1 = \Gamma_2 = 100$
The initial weighs of W	random within $[0, 0.3]$	random within $[0, 0.2]$
Gain matrices	—	$K_1 = 585$ $K_2 = 24$
Other parameters	$\theta = 1.5$	$\sigma_1 = \sigma_2 = 0.02$

Table 2. The vital parameters of the hydraulic driving system.

Parameters	Value	Parameters	Value
Cylinder dead length(m)	0.23	cylinder stroke length(m)	0.1016
The hydraulic density (kg/m3)	$8.304e^{2}$	the hydraulic effective bulk modulus (s-1)	$1.517e^{9}$
m (kg)	40	P_L (MPa)	5.5
F_V (Ns/m)	10000	F_C (N)	4
τ (s)	0.0035	K_c (m3s/Pa)	$2.0e^{-11}$
$C_{in} + C_{ex}$	$2e^{-14}$	k_s (m/Ma)	1.54
A_1 (m2)	$3.25e^{-4}$	A_2 (m2)	$2.1e^{-4}$
l_0 (m)	0.28	K_q (m3 s·A)	$18.2e^{-3}$

4.2 Experiment

To further demonstrate the validity of the force tracking control system, experimental tests have been addressed in this section. The setup of the proposed approach for the LEPEX hydraulic driving system is described in Fig. 8. The hydraulic cylinder and servo valve are self-made to meet the specific requirements such as maximum torque, minimal mass, suitable length and so forth. The configuration of the computing center is P4/2.0G CPU, 2G memory, 250G hard disk with a 16-bit A/D convertor, a 16-bit D/A convertor and an amplifier, etc. The experiment results are reported in Fig. 9-12. It clearly shows that the tracking error in the experiment is 0.966N, a bit larger than that in the simulation.

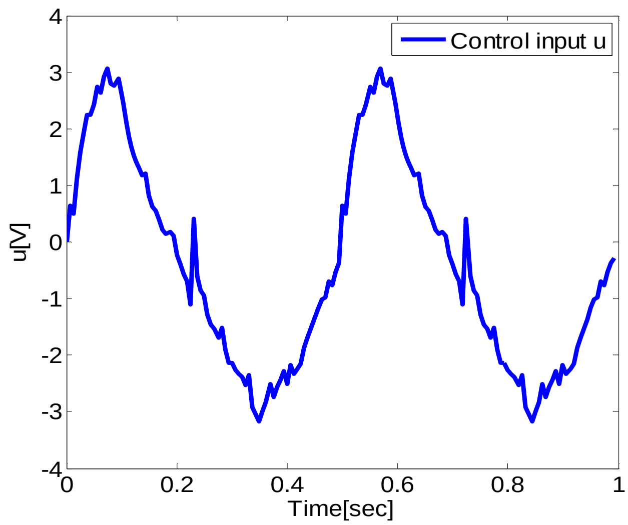

Fig. 7. The control signal u.

4.3 Results and discussion

Among the main characteristics of the proposed control scheme, we recall the possibility to require less sensors thanks to the use of RBF-NN observer. From the simulation results, it has been shown that the RBF-NN observer is robust (see Fig. 6) even though a limited number of neurons (that is 16) adopted, also the adaptive controller is effective in compensating for the nonlinearities of the system (see again Fig. 6).

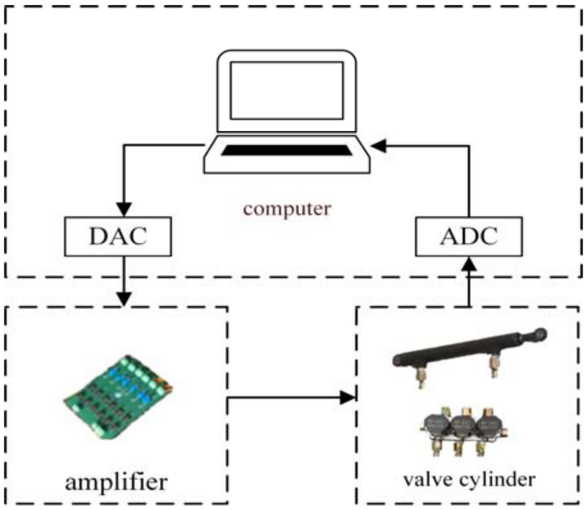

Fig. 8. Block diagram of LEPEX servo system for NN-observer-based force adaptive tracking control.

In view of the experimental results, the tracking error is slightly larger than that in the simulation. This is due to the presence of possible model uncertainties and measurement noise. This, on the other hand, shows that the proposed control scheme is also robust to model uncertainties and measurement noise.

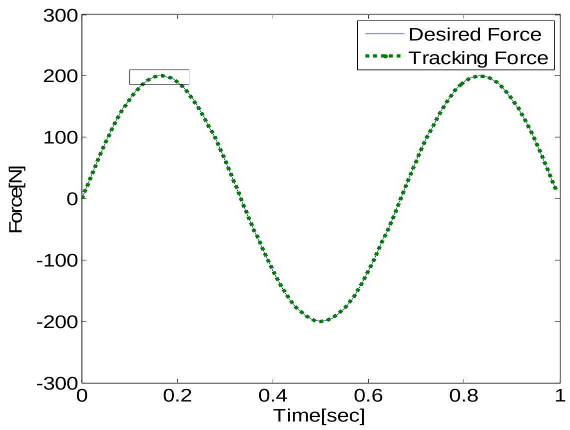

Fig. 9. Tracking trajectories with desired force of

$F_{Ld} = 200 \times \sin(3\pi t)$

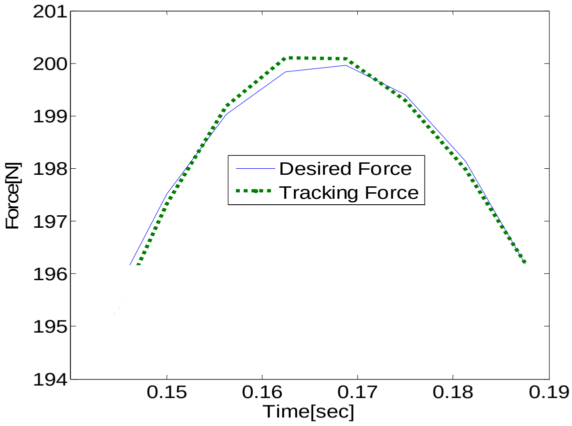

Fig. 10. The rectangular area marked in Fig. 9.

5. CONCLUSIONS

This paper presents a RBF-NN observer based force adaptive tracking controller for LEPEX. The approach allows to reduce the number of sensors thanks to the use of RBF-NN observer. Compatible with the observer, a NN adaptive output feedback controller has been designed to achieve the force tracking control goal. Moreover, rigorous Lyapunov analysis has been addressed to guarantee that the output variable of the control system, i.e., the load force converge to a computable set. From the simulation and experimental results, it has been shown that the proposed approach is effective in fulfilling the force control objective in presence of model nonlinearities and possible uncertainties. Future work will focus on the extension to the approach to switched control of LEPEX.

6. ACKNOWLEDGEMENTS

Part of this work was done at Social Robotics Laboratory, Department of Computer Science and Engineering, National University of Singapore. The author would like to thank Prof. Shuzhi Sam Ge for his kind guidance and fruitful suggestions.

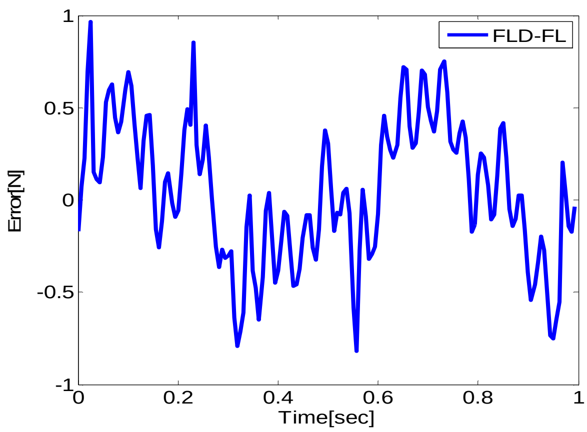

Fig. 11. The experimental force tracking error.

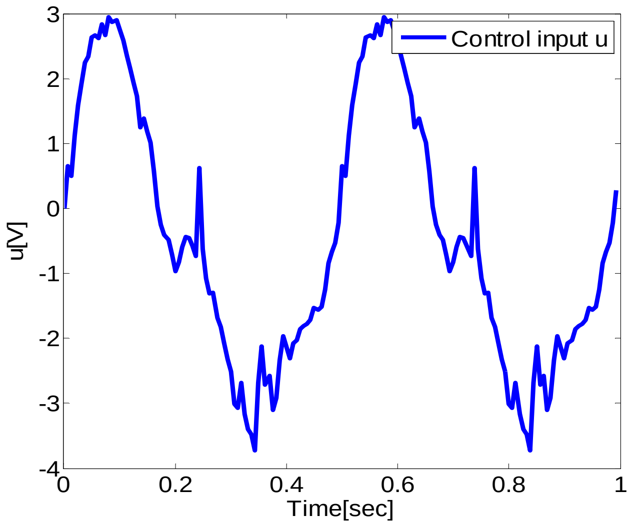

Fig. 12. The experimental control signal u .

REFERENCES

Abdollahi, F., Talebi, H.A., & Patel, R.V. (2006). A stable neural network-based observer with application to flexible joint manipulators. *IEEE Transactions on Neural Networks*, IEEE, 17, 118–129.

Abu-Khalaf, M., Lewis, F.L. (2005). Nearly optimal control laws for nonlinear systems with saturating actuators using a neural network HJB approach. *Automatica*, 41(5): 779–791.

Alleyne A., Liu, R. (2000). A Simplified Approach to Force Control for Electro-hydraulic Systems, *Control Engineering Practice*, 8(12),1347-1356.

Astolfi A, Karagiannis D, Ortega R (2008). *Nonlinear and adaptive control with applications*. Springer, London.

Banala S.K., Kim S.H., Agrawal S.K., et al (2009). Robot assisted gait training with active leg exoskeleton (ALEX). *IEEE Transactions on Neural Systems and Rehabilitation Engineering*, IEEE, 17: 2–8.

Chantranuwathana, S., Peng, H. (2004). Adaptive robust force control for vehicle active suspensions. *International Journal of Adaptive Control and Signal Processing*. 12(2): 83–102.

Chu, A., Kazerooni, H., & Zoss, A. (2005). On the biomimetic design of the berkeley lower extremity exoskeleton (BLEEX). In *Robotics and Automation*, 2005. ICRA 2005. *Proceedings of the 2005 IEEE International Conference on* (pp. 4345-4352). IEEE.

Ge, S. S., Lee, T.H., Harris, C.J. (1998). Adaptive neural network control of robotic manipulators, *Series in robotics and intelligent systems*, World Scientific.

Ge, S.S.; Ren, B., Tee, K.P., Lee, T.H. (2009). Approximation-based control of uncertain helicopter dynamics, *IET Control Theory and Applications*, 3(7):941-956.

Ge S. S., Wang C. (2014). Adaptive neural control of uncertain MIMO nonlinear systems[J]. *IEEE Transactions on Neural Networks*, 15(3):674-692.He W., Ge S.S., Li Y., Chew E, and Ng S.Y. (2015). Neural Network Control of a Rehabilitation Robot by State and Output Feedback, *Journal of Intelligent & Robotic Systems*, 80(1):15-31.

Gupta A., O'malley M.K., Patoglu V., et al (2008). Design, control and performance of ricewrist: a force feedback wrist exoskeleton for rehabilitation and training. *The International Journal of Robotics Research*, 27: 233–251.

Ho, T. H., & Ahn, K. K. (2010). Modeling and simulation of hydrostatic transmission system with energy regeneration using hydraulic accumulator. *Journal of mechanical science and technology*, 24(5), 1163-1175.

Huang Y., and Jiang H. (2015). Neural network observer-based optimal control for unknown nonlinear systems with control constraints, *International Joint Conference on Neural Networks*.

Huang Y, Liu D., and Wei Q. (2013). Convergence analysis of continuous-time systems based on feedforward neural networks, *IEEE International Symposium on Circuits and Systems*, IEEE, 2095-2098.

Igelnik, B., & Pao, Y.H. (1995). Stochastic choice of basis functions in adaptive function approximation and the functionallink net. *IEEE Transactions on Neural Networks*, 6, 1320– 1329.

Jagannathan, S. (2006). *Neural network control of nonlinear discrete-time systems*. Boca Raton: CRC Press.

Kazerooni H., Racine J.L., Huang L.H., et al (2005). On the control of the berkeley lower extremity exoskeleton (BLEEX). In: *Proceedings of the 2005 IEEE international conference on robotics and automation*, Barcelona, IEEE, pages4364–4371.

Kazerooni H., Steger R. (2006). The Berkeley Lower Extremity Exoskeleton, *IEEE/ASME Transactions on Dynamic Systems, Measurement, and Control*, IEEE, 128(14):14-25.

Kilic E., Dolen M., etc. (2012). Accurate pressure prediction of a servo-valve controlled hydraulic system, *Mechatronics*. 22(9): 997–1014.

Kobayashi H., Ozawa R. (2003) Adaptive neural network control of tendon-driven mechanisms with elastic tendons. *Automatica*. 39(9):1509–1519.

Lee H., Kim W., Han J., et al (2012). The technical trend of the exoskeleton robot system for human power assistance[J]. *International Journal of Precision Engineering and Manufacturing*, 13(8): 1491-1497.

Lewis, F.L., Jagannathan, S., & Yesildirek, A. (1999). *Neural network control of robot manipulators and nonlinear systems*. London: Taylor & Francis.

Lewis, F.L., & Vrabie, D. (2009). Reinforcement learning and adaptive dynamic programming for feedback control. *IEEE Circuits and Systems Magazine*, 9, 32–50.

Li Y., Ge S.S., Zhang Q. and Lee T.H. (2013). Neural networks impedance control of robots interacting with environments, *IET Control Theory and Applications*, 7(11):1509-1519.

Nagarajan, U., Aguirre-Ollinger, G., & Goswami, A. (2016). Integral admittance shaping: A unified framework for active exoskeleton control, *Robotics and Automation Systems*, 75:310-324.

Pan, D., Gao F., and Miao Y. (2014). Dynamic research and analyses of a novel exoskeleton walking with humanoid gaits. *Proceedings of the Institution of Mechanical Engineers Part C Journal of Mechanical Engineering Science*. 228(9):1501-1511.

Park, S.H., Han, S.I. (2010). Robust-tracking control for robot manipulator with deadzone and friction using backstepping and RFNN controller, *IET Control Theory and Applications*, 5(12):1397-1417.

Rito, G. D., Denti E., and Galatolo R. (2006). Robust Force Control in a Hydraulic Workbench for Flight Actuators. *IEEE Proc.*, Munich, Germany, Oct. : 807-813.

Sharma, M., and Verma, A. (2012). Wavelet Neural Network Observer Based Adaptive Tracking Control for a Class of Uncertain Nonlinear Delayed Systems Using Reinforcement Learning. *International Journal of Intelligent Systems and Applications*. 38:1011-1023.

Sharma,M., and Verma A. (2013). Wavelet reduced order observer-based adaptive tracking control for a class of uncertain delayed non-linear systems subjected to actuator saturation using actor-critic architecture. *International Journal of Automation and Control*. 11(3):496-502.

Song, S., Zhang X. and Tan Z. (2014). RBF neural network based sliding mode control of a lower limb exoskeleton suit, *Strojniški vestnik-Journal of Mechanical Engineering* 60(6) :437-446.

Steger R. (2005). On the Control of the Berkeley Lower Extremity Exoskeleton (BLEEX). *Proceedings of the 2005 IEEE International Conference on Robotics and Automation*, IEEE,pages4353-4360.

Xiong Y., Liu D., and Wang D. (2014). Reinforcement learning for adaptive optimalcontrol of unknown continuous-time nonlinear systems with input constraints. *International Journal of Control*. 87(3):553-566.

Yanan Li, Shuzhi Sam Ge, Qun Zhang, Tong Heng Lee (2013). Neural networks impedance control of robots interacting with environments. *IET Control Theory and Applications*, 7(11):1509-1519.

Zoss, A. B., Kazerooni, H., & Chu, A. (2006). Biomechanical design of the Berkeley lower extremity exoskeleton (BLEEX). *IEEE/ASME Transactions On Mechatronics*, 11(2), 128-138.